

# Canopy gaps and associated losses of biomass - combining UAV imagery and field data on a Central Amazon forest

Adriana Simonetti<sup>1,2</sup>, Raquel Fernandes Araujo<sup>2</sup>, Carlos Henrique Souza Celes<sup>2</sup>, Flávia Ranara da Silva e Silva<sup>1,2</sup>, Joaquim dos Santos<sup>2</sup>; Niro Higuchi<sup>2</sup>, Susan Trumbore<sup>3</sup> and Daniel Magnabosco Marra<sup>3</sup>

5 <sup>1</sup>Programa de Pós-graduação em Ciências de Florestas Tropicais, Instituto Nacional de Pesquisas da Amazônia, Manaus, 69060-062, Brazil

<sup>2</sup>Laboratório de Manejo Florestal, Instituto Nacional de Pesquisas da Amazônia, Manaus, 69060-062, Brazil

<sup>3</sup>Biogeochemical Processes Department, Max Planck Institute for Biogeochemistry, Jena, 07745, Germany

10 *Correspondence to:* Adriana Simonetti (adrianasimonettip@gmail.com) and Daniel M. Marra (dmarra@bgc-jena.mpg.de)

**Abstract.** Understanding mechanisms of tree mortality and the dynamics of associated canopy gaps is relevant for robust estimates of carbon balance in forests. We combined monthly RGB images acquired from an unmanned aerial vehicle with field surveys to identify gaps in an 18-ha plot installed in an old-growth Central Amazon forest. In addition to detecting, we measured the size and shape of gaps, and analyzed their temporal variation and correlation with rainfall over a period of 28 months. We further described associated modes of tree mortality (i.e., snapping, standing dead and uprooting) or branch fall and quantified associated losses of biomass. In total, we detected 32 gaps either in the images and field ranging in area from 9 m<sup>2</sup> to 835 m<sup>2</sup>. Relatively small gaps (<39 m<sup>2</sup>) associated with branch fall were the most frequent (11 gaps). Out of 18 gaps for which both field and imagery data were available, three could not be detected remotely. Gaps observed in the field but not captured on the imagery were relatively small and mainly formed by the fall of branches from live and standing dead trees. Our data show that ~17% of the tree-mortality and branch-fall events only affect the lower canopy and the understory of the forest, and are likely neglected by assessments of top of the canopy. Regardless the detection method, the size distribution of gaps was better captured by a Lognormal function for gaps starting from the smallest detected size (9 m<sup>2</sup> for field and 10 m<sup>2</sup> for UAV imagery). The Weibull function was the second-best fit for gaps larger than 10 m<sup>2</sup> and the best fit for gaps larger than 25 m<sup>2</sup>. As confirmed by our detailed field surveys, we believe that this pattern was not biased by gaps possibly undetected from image data. Although not related to differences in gap size, the main modes of tree mortality partially explained losses of biomass. Moreover, the rate of gap area formation was positively correlated with the frequency of extreme rainfall events, which may be related to a higher frequency of storms propagating extreme rain and destructive wind gusts. The correlation between modes of tree mortality and size of gap with associated losses of biomass provide evidence on the relative importance of small-scale events of tree mortality and branch fall as processes that contribute to landscape patterns of canopy disturbance and carbon balance in Amazon forests. While combining remote sensing with field data provided a robust assessment of gap dynamics and related losses of biomass, our results shall not be extrapolated beyond our study region. Future investigation may be carried in sites with varying forest attributes and environmental characteristics. Apart from improving landscape

assessments of carbon balance, regional information on gap dynamics and associated mechanisms of gap formation are relevant  
35 to address forest responses to altered disturbance regimes resulting from climate change.

## 1 Introduction

Tropical forests store ~25 % of terrestrial biomass carbon stocks (Pan et al., 2013). The maintenance of these stocks depends  
on dynamic processes that regulate the growth and mortality of trees (Brienen et al., 2015; McDowell et al., 2018; Frelich,  
40 2016). Reports of increased tree mortality in tropical and temperate regions raise questions about the influence of climate  
change on the dynamics and functioning of old-growth forests (Laurance et al., 2004; Phillips and Gentry, 1994; Allen et al.,  
2015). In the tropics, climate change is related to increased frequency and intensity of extreme events, such as convective  
storms and droughts (Feng et al. 2023; Tan et al., 2015; Allen et al., 2015; IPCC, 2021) that can increase rates of tree mortality  
and/or branch fall, thereby altering patterns of forest biomass and carbon (Laurance et al., 2004; Chambers et al., 2013;  
45 McDowell et al., 2018). Understanding mechanisms of tree-mortality and gap formation is fundamental to upscale estimates  
of carbon balance and to anticipate the response of forests to climate scenarios (Clark et al., 2017; Leitold et al., 2018).

Gaps are natural openings in the forest canopy caused by falling trees and/or branches (Brokaw, 1982; Whitmore, 1989). Such  
disturbances exert great influence on the dynamics and functioning of tropical forests, as they alter structure (Kellner et al.,  
2009), natural regeneration (Grubb, 1977; Kellner and Asner, 2014; Marra et al. 2014a), species diversity and composition  
50 (Denslow, 1987; Magnabosco Marra et al., 2014b, 2018), soil carbon and nutrients (Santos et al., 2016; Vitousek and Denslow,  
1986), and productivity (Baker et al., 2004). The size of gaps can vary from a few square meters to thousands of hectares,  
depending on the mechanism of formation (Nelson et al., 1994; Fontes et al., 2018; Magnabosco Marra et al., 2018; Esquivel-  
Muelbert et al., 2020; Araujo et al., 2017, 2021). The size and shape of gaps define the amount of light and other key resources  
during succession (Denslow, 1980, 1987; Schliemann and Bockheim, 2011). Apart from related to mechanisms of formation,  
55 the size and shape of gaps can be influenced by local climate and topography, soil and forest structure and species composition  
(Denslow, 1987; Araujo et al., 2021; Cushman et al., 2022). Thus, assessing the size distribution of gaps provides information  
on key processes regulating forest structure and diversity, and related functions (Jucker, 2022). Large-scale windthrows are a  
frequent disturbance in the Amazon. Although with some surviving trees, gaps opened by extreme rain and wind can have  
areas greater than 3,000 hectares (Nelson et al., 1994; Espírito-Santo et al., 2014; Negrón-Juárez et al., 2010, 2018, 2023).  
60 Recent studies reported windthrow hotspots (Negrón-Juárez et al., 2023), and that their frequency is regulated by atmospheric  
phenomena that are highly sensitive to climate change, such as the potential energy available for convection (CAPE) (Feng et  
al., 2023).

In the Central Amazon region, extreme wind gusts and precipitation are important mechanisms of tree damage and mortality  
(Nelson et al. 1994; Chambers et al., 2013; Magnabosco Marra et al., 2018; Negrón-Juárez et al., 2018, 2023). A study  
65 monitoring tree mortality over five decades in a Central Amazon forest found that trees died more frequently in wet months,

even during drought years (Aleixo et al., 2019). A positive correlation between precipitation and tree mortality was also reported for an adjacent area (Fontes et al., 2018). A regional study based on 12 years of satellite data found that major windthrows (visible on Landsat) in Central Amazon occurred more frequently between September and February, which are months marked by heavy rainfall (Negrón-Juárez et al., 2017). These studies support that a greater number of gaps can be expected during the rainy season, when convective storms propagating extreme wind gusts are more frequent.

In the field, a gap can be defined by an opening in the forest canopy extending from the upper stratum to an average height of two meters above ground (Brokaw, 1982). Traditionally, studies of gap dynamics and geometry (e.g., area, perimeter and shape) have relied on observations made as part of forest inventories (Brokaw, 1982; Hubbell et al., 1999). However, gap-forming events can be stochastic and obtaining robust information on their frequency and geometry from often relatively low number of plots surveyed infrequently is a challenging task (Fontes et al., 2018).

In recent years, studies of gap frequency and geometry have been conducted using fine-scale remote sensing, which allows for inferences across larger spatial scales (Getzin et al., 2014; Araujo et al., 2021; Asner et al., 2013; Dalagnol et al., 2021), at high accuracy and spatial resolution (Senf, 2022; Froking et al., 2009). However, optical remote sensing methods usually have a limited detection of the lower canopy of dense forests. In the Amazon, studies using intermediate spatial-resolution remote-sensing data have shown that small gaps are more frequent than relatively larger events, such as large gaps associated with convective storms (Nelson et al., 1994; Chambers et al., 2013; Araujo et al., 2017). However, the use of these data such as Landsat (30 m x 30 m pixel, 0.09 ha) do not allow mapping the smaller and more frequent disturbances (e.g., < 0.1 ha), including those only affecting the lower canopy of the forest. As demonstrated for the region of Manaus (Brazil), Landsat images are only sensitive in detecting mortality events involving from 6 to 8 fallen trees (Negrón-Juárez et al., 2011; Chambers et al., 2013). This mismatch between the monitoring of gap dynamics using forest inventory and satellite data highlights the lack of knowledge on mechanisms of formation of relatively smaller and more frequent gaps, and thus of their influence on landscape patterns of forest dynamics and biomass balance (Negrón-Juárez et al., 2011).

An alternative to assess the full gradient of gap size and geometry is the photogrammetry computed from unmanned aerial vehicle (UAV) imagery, commonly known as drones. In addition to a more detailed description of size and geometry, successive imaging acquired with UAVs makes it possible to monitor gap dynamics at higher spatial and temporal resolutions than that provided by satellite imagery (e.g., high cloud cover and relatively long revisiting times) (Getzin et al., 2014; Araujo et al., 2021; Senf, 2022). Still, the monitoring of gap dynamics using high spatial and temporal resolution imagery must be validated with field data.

Here we combined continuous forest inventories with UAV high-resolution photogrammetry to quantify the relative contribution of mechanisms of gap formation such as different modes of tree mortality and branch fall, and to compute associated losses of biomass in an 18-ha Amazon forest. The combination of high spatial-resolution imagery and field data offered us an unique opportunity to describe the seasonality of tree-mortality events and possible interactions with extreme weather events and their relevance for the maintenance of carbon stocks (Esquivel-Muelbert et al., 2020).. We addressed the following questions: i) How sensitive is RGB photogrammetry acquired with UAV for the detection of gaps compared with

100 forest inventory data? ii) Is there a difference in the size distribution and geometry of gaps measured with photogrammetry and forest inventory? iii) Are gap geometry and biomass losses influenced by modes of tree mortality? iv) Is the rate and size of gap formation related to rainfall?

## 2 Methods

### 2.1 Study area

105 The study was conducted on a permanent plot (2°36'47" S; 60°08'41" W) monitored within the Wind–Tree Interaction Project (INVENTA) and the Amazon Tall Tower Observatory (ATTO) (Fig. 1a). This plot (hereafter referred to as INVENTA plot) is located at the *Estação Experimental de Silvicultura Tropical* (EEST) from the *Instituto Nacional de Pesquisas da Amazônia* (INPA), a reserve with 21,000 ha of contiguous old-growth forest (Fig. 1b). The EEST is accessible via the local road ZF-2, located at km 50 of the BR-174 highway north of Manaus, Brazil (Fig. 1c). The INVENTA plot has a size of 18 ha (600 m x  
110 300 m) and is divided into 20 m x 20 m subplots (total of 450 subplots), which are subdivided into four 10 m x 10 m quadrats (total of 1,800 quadrats). The INVENTA plot was established in 2000 as part of the Jacaranda Project (Pinto et al., 2003). At the time it started, all trees, palms and lianas with DBH (diameter at breast height, 1.3 m)  $\geq 5$  cm were recorded. In 2017, prior to the start of INVENTA, all trees and palms with DBH  $\geq 10$  cm were remeasured.

The canopy trees in our study region are  $28.65 \text{ m} \pm 0.46 \text{ m}$  tall (mean  $\pm$  standard deviation) (Araujo, 2019). The forest  
115 understory and canopy are dense and closed. The richness of 10 cm DBH trees can exceed 280 species  $\text{ha}^{-1}$  (Oliveira and Mori, 1999). The INVENTA plot has an undulating topography typical of the region, including areas of plateau, slope and valley. The mean annual precipitation and temperature in the Manaus region are  $2,231 \pm 118 \text{ mm year}^{-1}$  (mean  $\pm$  95 % confidence interval) and  $26.9 \pm 0.17 \text{ }^\circ\text{C}$ , respectively (1970-2016 period) (Magnabosco Marra et al., 2018). The region experiences three consecutive months (mostly commonly from July to September) with less than 100 mm of rainfall (Negrón-Juárez et al., 2017;  
120 Wu et al., 2016).

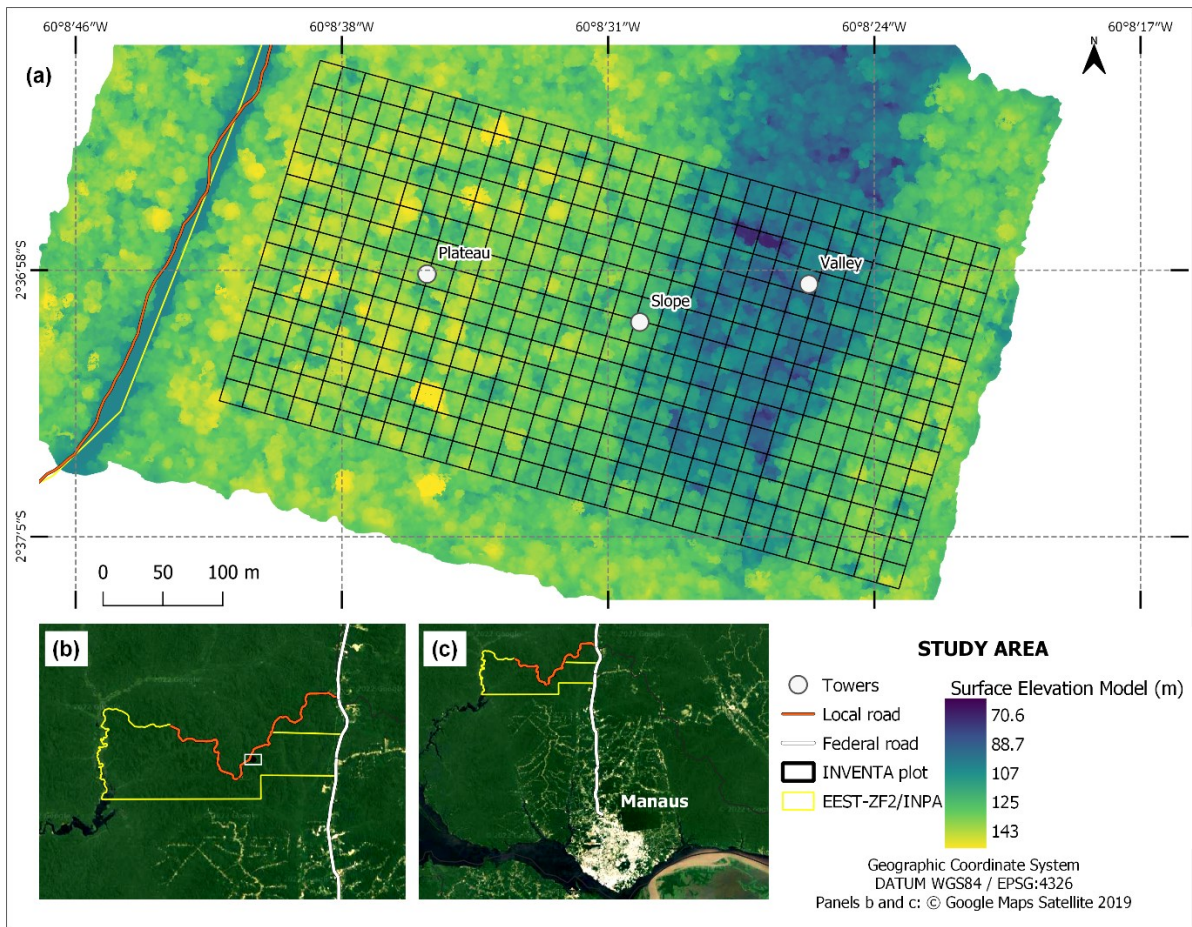


**Figure 1: Study area (INVENTA plot) with an area of 18 ha (300 m x 600 m), located ~50 km north of Manaus, Central Amazon, Brazil. Elevation refers to the canopy surface model generated from photogrammetry of images obtained with UAV.**

## 2.2 Acquisition and processing of remote sensing data

125 Imagery data were collected monthly, between September 2018 and January 2021 (28 months), using a digital RGB camera  
 deployed on *DJI Phantom 3* and *4* UAVs (see collection period in Table S1). The flight plans were programmed using the *DJI*  
*Ground Station* application installed on a tablet device (Apple, model A1489), which was connected to the aircraft remote  
 control and configured for automated flight from predefined waypoints. The camera lens has a Field of View (FOV) angle of  
 94°, and the pictures generated have a resolution of 12 Mp, with maximum dimensions of 4,000 pixels x 3,000 pixels. The  
 130 overflights were performed at 100 m height above the ground, with an approximate speed of 9.9 m s<sup>-1</sup> in order to generate  
 images with ~100 m width at canopy height. Photographs were captured every 2 seconds with 85 % longitudinal overlap, and  
 70 % lateral overlap with respect to the ground. The camera was calibrated on each flight to reduce the effects of varying  
 illumination within and between flights. To ensure homogeneous images and diffuse lighting conditions throughout the studied

period, whenever possible, flights were performed in mid-morning and/or late afternoon (further details on data acquisition are available in Text S1).

The acquired photos were processed using *Agisoft Metashape* (Version 1.5.2) (AGISOFT LLC., St. Petersburg, Russia). This software aligns photos using the Scale Invariant Feature Transformation (SIFT) algorithm (Lowe, 2004), which allows for ratifying photos with a bending angle greater than three degrees. Through this procedure photos were aligned from overlapping common features (i.e., textures). Further, these aligned points were given X, Y, Z coordinates and the parallax effect seen on the overlapping photos was used for reproducing the stereoscopic (3D) view based on the Structure from Motion (SfM) method. After creating the 3D point network, a dense cloud of XYZ points was generated to fill empty spaces (i.e., Dense Point Cloud). From the Dense Point Cloud, a digital surface model (DSM) and an orthomosaic were generated. The DSM is a digital geographic dataset that represents surface elevations with horizontal and vertical (X, Y, Z) coordinates (Iglhaut et al., 2019). The orthomosaic reproduces the real dimensions of objects (Araujo et al., 2020), with horizontal spatial resolution ranging from 3 cm to 7 cm.

The orthomosaic and DSM were aligned vertically and horizontally using the georeferencing process from LiDAR data collected along transects as part of the EBA project (Ometto et al., 2021), which covered the INVENTA plot. The workflow consisted of creating a georeferenced project based on control points extracted from LiDAR. Subsequential flights were matched using the ‘Align Chunks’ tool available in *Agisoft Metashape* (more detail on the process in Text S2).

### 150 **2.2.1 Detection of canopy gaps**

Canopy gaps within the UAV images were identified through the combination of DSM change analysis, visual interpretation of the orthomosaics (Fig. 2) and field data. Initially, we resampled the pixel resolution of photos to 1 m, and the difference-image was calculated for all pairs to obtain a raster product (i.e., difference-image) describing changes in canopy height among time intervals.

155 In order to compare our data with previous studies, the area of the identified gaps was computed as the region where the canopy lost more than 10 m in height over continuous areas larger than 5 m<sup>2</sup> and with an area/perimeter ratio greater than 0.6. This was also the smallest gap size reported in previous studies (Runkle and Yetter, 1987; Getzin et al., 2014). By computing the area/perimeter ratio, we were able to remove artifacts associated with slight changes on the positions of individual trees in subsequential pairs of images, both due to wind-driven canopy shifts and changes in tree alignment (Araujo et al., 2021).  
160 Therefore, the criterion for gap identification was based on the analysis of gap size and shape. Finally, successive pairs of orthomosaics covering subplots (400 m<sup>2</sup>) were visually checked. When necessary, we edited the pre-delineated polygons by removing false gaps related to image noise (Araujo et al., 2021).

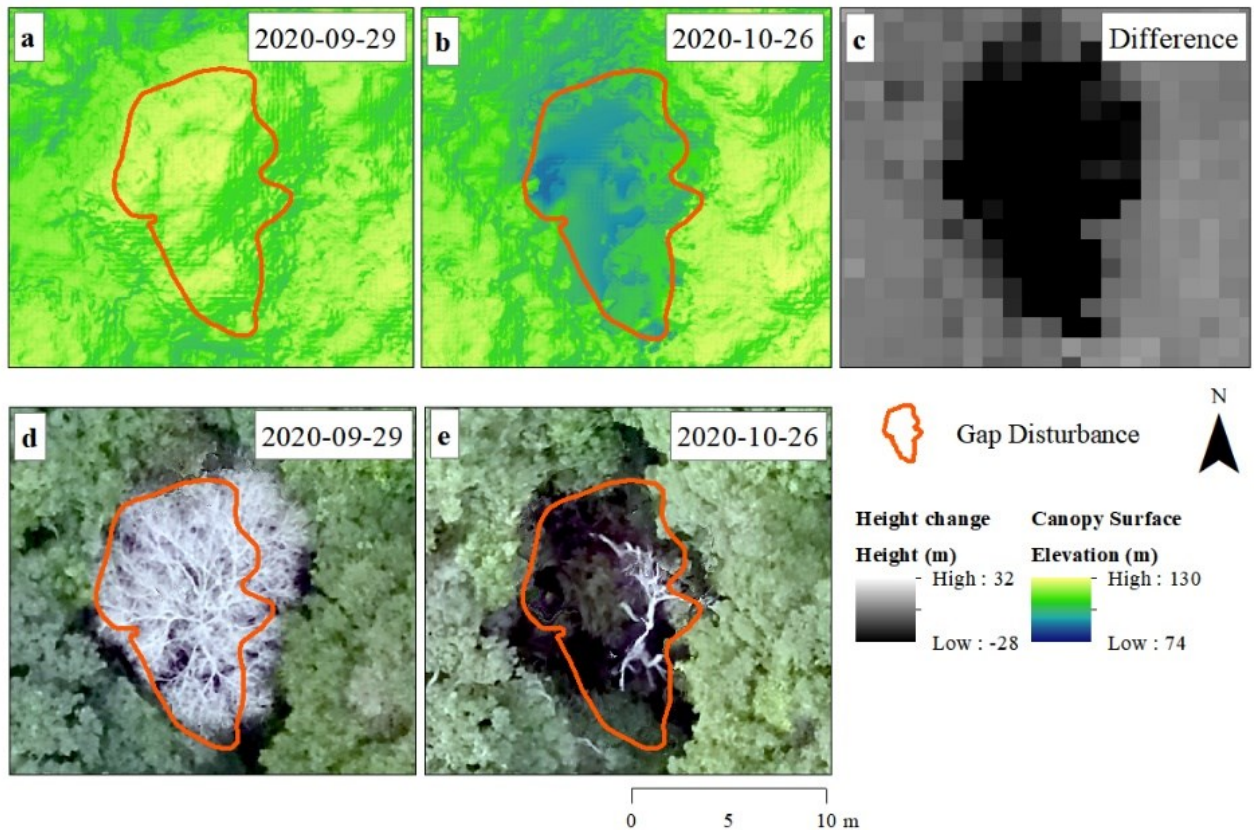


Figure 2: Canopy gaps identified from surface models and orthomosaics computed from photogrammetric analyses of UAV imagery. Elevation model for a studied gap on two successive flights from 29<sup>th</sup> September 2020 (a) and 26<sup>th</sup> October 2020 (b). The difference in surface elevation between flights (black area) indicates a reduction in canopy height (c). RGB orthomosaics from the same dates (d, e).

### 2.3 Field surveys for evaluating remotely sensed gaps

Field data were collected bimonthly (section 2.3.1) and included the identification and description of gaps formed between November 2019 and January 2021 (14 months) (see collection period in Table S1). Initially, we identified and marked on the images all gaps formed before the studied period to create a reference baseline. The identification and description of gaps in the field were conducted by walking the entire plot. To minimize errors, this task was always carried out by the same team using existing trails 10 m distant from each other to ensure precise counting and description of gaps.

We used the definition by Brokaw 1982, i.e., gap in the forest canopy extending from the upper stratum to an average height of two meters above ground) to compute and measure gaps in the field. This is a classical and practical method, which allows comparing our findings with those from fundamental work conducted in other tropical forests. In addition to confirming the



gaps identified in the images, the field surveys included detailed walking of the entire plot to identify gaps possibly not detected remotely. The delimitation of gaps in the field was made by taking the coordinates (distance and azimuth) from the near center to the edge of the gap. We defined the boundaries of gaps by projecting the canopy aperture to the ground. For distance and azimuth measurements, a *TruPulse* 360B laser rangefinder (Laser Technology) was used. The center of the gap was defined in the field, and coordinates were collected by averaging Global Navigation Satellite System (GNSS) navigation points. From the center of the gap, the acquisition of eight directions and distances to the gap boundary was done counterclockwise, with the first measurement pointing north (360°/0°). The data from each gap was vectorized in QGIS Geographic Information System (version 3.4.13) (Open Source Geospatial Foundation Project. <http://qgis.osgeo.org>) environment from the center point. We then calculated geometric features, including gap area, perimeter, and shape complexity index.

### 185 **2.3.1 Mechanisms of gap formation and biomass estimation**

After delimiting gaps, we measured forest-structure attributes. For dead trees, the tag number, number of plot and sub-plot, diameter at breast height (DBH, 1.3 m above the ground) and the mode of mortality were recorded. We described modes of tree mortality based on previous studies conducted in our study region (Magnabosco Marra et al., 2014b; Ribeiro et al., 2016): (i) Standing dead - trees without leaves and/or presence of sap in the trunk; standing-dead trees can form or expand gaps through falling branches or the later breakage of the main stem; (ii) Snapping – trees that died from the mechanical rupture of the stem, with sap often still present at the portion connected to the roots, exposed wood fibers and no clear damaged or exposed roots; (iii) Uprooting - uprooted trees with the main trunk usually intact and still connected to the crown.

Tree biomass was estimated using a simple-entry allometric equation calibrated locally (Magnabosco Marra et al., 2016). For branches with diameter  $\geq 5$  cm, the volume was obtained by cubing combining the Smalian (measuring diameters at the base and top) and Hohenald (relative section length division) cubing methods (Lima et al., 2012; Gimenez et al., 2017). Most of the branches had no fresh vegetative material that allowed taxonomical identification to the species level. Thus, we estimated branch biomass by multiplying the measured volume of branches by the mean wood-density value compiled for our study region (0.735 [0.480,1.000], being mean wood density [ $\text{g cm}^{-3}$ ], minimum and maximum, respectively) (Magnabosco Marra et al., 2016).

### 200 **2.4 Rainfall data**

Rainfall data covering the studied period were acquired from a rain gauge installed at the EEST/INPA and located about 2 km from the INVENTA plot. Total daily precipitation was annotated manually. The dry season was defined as the months in which total rainfall was lower than the monthly average throughout the monitored period. For that, we used a threshold rainfall of  $< 200$  mm (July, August, September, and October) because there were no consecutive months with rainfall  $\leq 100$  mm (Negrón-Juárez et al., 2017; Wu et al., 2016) (Fig. S1) during the period of this study. We also identified days with extreme rain events, which were defined as those when the accumulated precipitation was higher than the 99<sup>th</sup> percentile calculated for the entire studied period.



## 2.5 Data analysis

### 2.5.1 Remote sensing and field detection of gaps

210 Field data acquired by using the definition of Brokaw, 1982 was considered as ground truth. To accomplish with this goal, we used a confusion matrix for assessing the accuracy of our remote method of gap detection. Further, we calculated the percentiles of accuracy (a), precision (p), recall (r), and F1 Score (F) (Eqs. 1 – 4) (Dalagnol et al., 2021), where TP is true positive, TN is true negative, FP is false positive and FN is false negative:

$$215 \quad \textit{Accuracy} (a) = ((TP+TN) /n) *100 \quad (1)$$

$$\textit{Precision} (p) = (TP/(TP+FP)) *100 \quad (2)$$

$$\textit{Recall} (r) = (TP/(TP+FN)) *100 \quad (3)$$

$$\textit{Score F1} (F) = (((2*p*r) / (p + r))) *100 \quad (4)$$

220 The total number of correct detections is expressed as percentile. The p percentile indicates the ratio of positive predictions performed correctly based on all positive predictions (including false ones). The r percentile is used to access the ratio of correct positive-predictions in relation to all positive predictions. The F1 Score (F) is the harmonic mean between p and r, i.e., the mean between the errors of commission and omission; higher F-values indicate higher agreement between gaps identified in the imagery data and observed in the field (ground truth).

### 225 2.5.2 Gap geometry

We quantified gap height and area from the three-dimensional structure of the forest canopy. Gaps formed during the period for which only the UAV monitoring was available, were validated during a single field-campaign. The area of these gaps was also measured according to Brokaw's (1982) method. We tested how height loss was correlated with the area of the gaps using Pearson's correlation. We used paired t-test to compare gap geometry calculated from our UAV imagery and field data.

230 We used both UAV imagery and field data to describe the size distribution of gaps. We then fitted three probability distributions: Exponential, Power-law (or Pareto), Weibull and Lognormal to determine which best described the size distribution of observed gaps. We used a bootstrap with 1,000 interactions for calculating the confidence interval of the different fits (Araujo et al., 2021a). The parsimony of the fitted models was assessed using the Akaike information criterion (AIC) (Burnham and Anderson, 2002). We also assessed the best fit using the Kolmogorov-Smirnov statistic to compare the  
235 maximum difference in the cumulative probability distributions between the observed and the fitted data (Carvalho, 2015). Fits were obtained by using absolute values of frequency (Araujo et al., 2021a). We tested the size class distributions from the smallest gap size found in both methods (9 m<sup>2</sup> and 10 m<sup>2</sup>, for field data and UAV imagery, respectively). We also fitted the distribution model only for gaps ≥ 25 m<sup>2</sup> to test for possible differences related to the relatively higher proportion of small-sized gaps in our data set.

### 240 **2.5.3 Mechanisms of gap formation, biomass losses and structure of gaps**

Combining high-resolution remote sensing with forest inventory data allowed us to identify and differentiate between gaps formed by the death of single trees, tree clusters and branch fall. We counted and determined the area of gaps formed by each of these mechanisms. The main mode of tree mortality was determined from detailed observations as described in subsection 2.3.1. We tested for possible differences in area and released biomass among mechanisms of gap formation using Analysis of  
245 Variance (ANOVA); p-values were computed based on two-tailed.

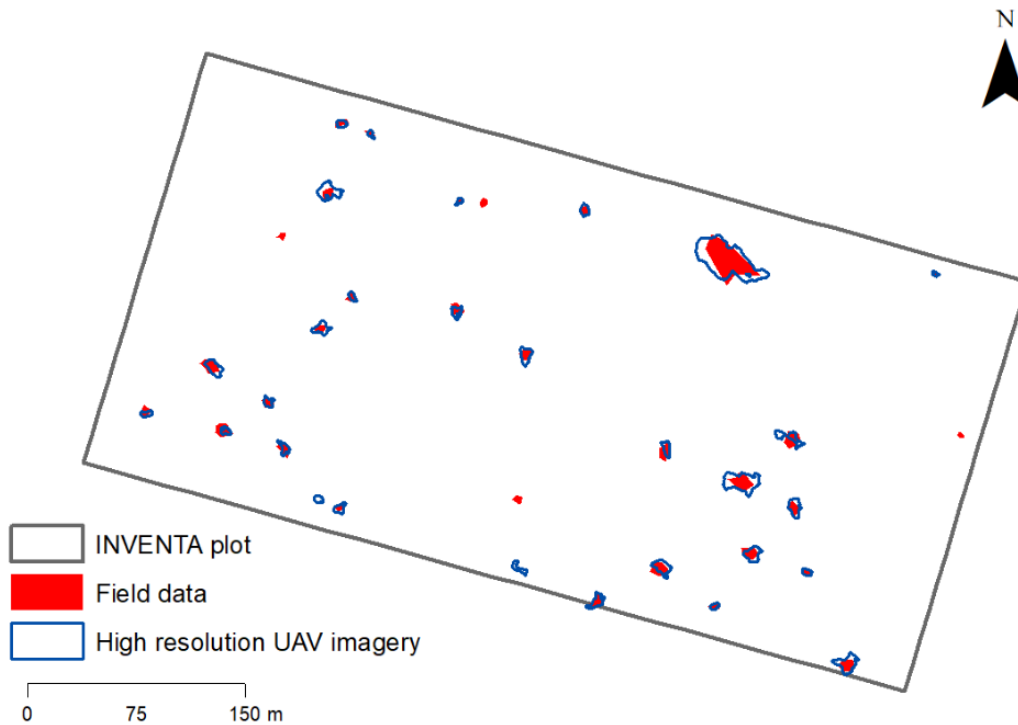
### **2.5.4 Correlations between gap frequency and area with precipitation**

We assessed the correlation of gap frequency and area with cumulative precipitation and extreme rainfall events using data acquired locally (see section 2.4). We further calculated the rate of gap area formation by dividing the summed area of all gaps by the duration (in days) of respective time intervals during which the gaps were observed (11-80 days). We expressed the rate  
250 of gap area formation in hectares per month. Gap frequency rate was also computed from the summed area over the different time intervals and was expressed in percentage per month. The temporal variation of gap area and frequency were normalized by the time in months between each pair of images. We correlated these variables using Pearson correlation.

## **3 Results**

### **3.1 Sensitivity of gap detection**

255 We remotely detected 32 gaps formed between September 2018 and January 2021 (Fig. 3). Out of that, 14 gaps were formed during the monitoring period for which no simultaneous field data were acquired. Another 18 gaps were formed during the period for which we conducted both remote and field monitoring (November 2019 to January 2021).



260 **Figure 3: Map including the location of canopy gaps identified with UAV photogrammetry and inventory plot surveys (“field data”) in the INVENTA plot (total area of 18-ha) located in Central Amazon, Brazil, during the period from 18<sup>th</sup> September 2018 to 19<sup>th</sup> January 2021.**

For the 18 gaps for which field (true value) and UAV data were available, 14 gaps were detected using both methods; three gaps were only detected in the field and one was only detected in the imagery (Table S2). The accuracy, precision, recall  
 265 sensitivity and F1 score obtained with our remote sensing UAV method were 77.78 %, 93.33 %, 82.36 % and 87.50 %, respectively.

The three gaps detected exclusively from field data were formed by the fall of standing dead trees (total area of 15 m<sup>2</sup> and 26 m<sup>2</sup>) and branches (20 m<sup>2</sup>). These gaps were not visible on either the difference images or the orthomosaics, which indicates that there was no traceable change in the upper canopy of the forest. The single gap only detected from imagery data was  
 270 formed by the partial loss of the crown of a standing dead tree. Importantly, this gap does not fit the definition by Brokaw (1982), in which gaps are considered as openings that extends from the upper canopy to the understory (i.e., at least two meters above the ground).

### 3.2 Patterns of gap geometry

The size of gaps identified from imagery and field data varied from 10.37 m<sup>2</sup> to 834.65 m<sup>2</sup> and from 9.59 m<sup>2</sup> to 580.65 m<sup>2</sup>, respectively (Table 1, Fig. S2a). The differences between the smallest and largest gaps detected with the two methods were 1.39 m<sup>2</sup> and 254 m<sup>2</sup>, respectively. Our data provide no evidence for strong differences in gap area between methods ( $p=0.8544$ ). Nonetheless, gap perimeter and shape complexity index (GSCI) varied significantly between methods ( $p=0.01019$  and  $p \leq 0.001$ , respectively) (Table S3).

280 **Table 1.** Geometric attributes of gaps detected over a period of 28 months in the INVENTA plot, Central Amazon, Brazil.

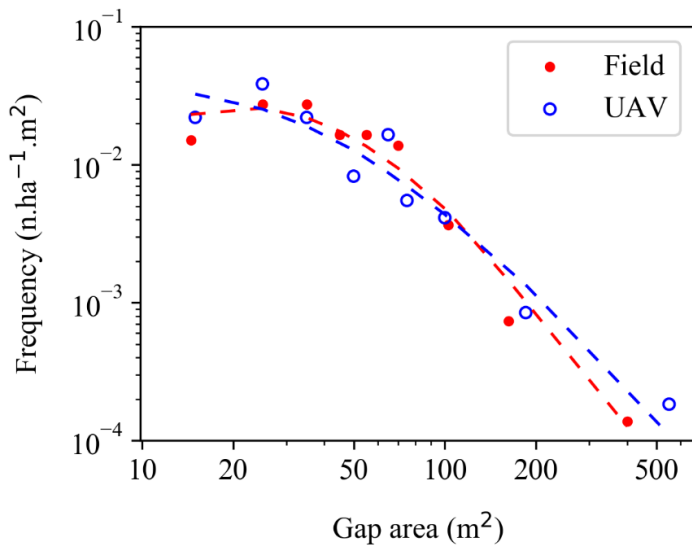
Method	Number of gaps	Size range (m <sup>2</sup> )	Mean gap size (m <sup>2</sup> ) ± IC (95 %)	Median gap size (m <sup>2</sup> )	Mean gap perimeter (m) ± IC (95%)	GSCI <sup>1</sup> Mean/Max	Gap fraction <sup>2</sup> (%)	Annualized gap fraction (% year <sup>-1</sup> ) <sup>3</sup>
Field Data	31	9.59 - 580.65	68.50 ± 37.91	44.88	29.86 ± 6.92	1.13/1.35	1.09	0.60
UAV Imagery	30	10.37 - 834.65	80.07 ± 56.81	37.43	35.42 ± 9.22	1.28/1.6	1.36	

1- Gap Shape Complexity Index (GSCI = perimeter / sqrt (area 4  $\pi$ )), whose smallest reference value is 1.0 for describing a circle (Getzin et al., 2012, 2014); 2- Gap fraction is given by the sum of the area of gaps identified over the studied period of 28 months divided by the total monitored area (i.e., INVENTA plot / 18 ha); 3- Annual gap fraction is given by the sum of the area of identified gaps in an annual basis, (i.e., INVENTA plot / 18 ha / duration of study).

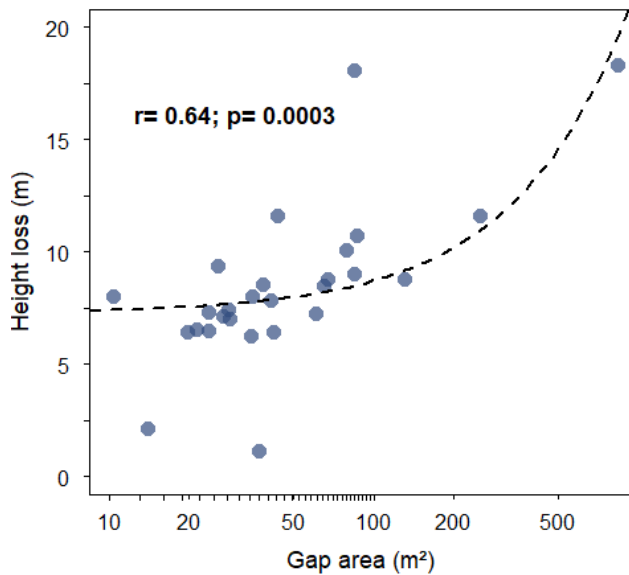
285

Approximately 50 % of gaps described within the 28 months for which field and imagery data were available had total area  $\leq 40$  m<sup>2</sup>. This result indicates that in our study site, relatively small gaps are the most frequent canopy disturbance (Fig. 4, and Table S4). Although more frequent, these relatively small disturbances accounted for only ~16 % of the cumulated gap area. Gap size was positively related to reductions in canopy height (Pearson  $r=0.64$ ;  $p=0.0003$ ) (Fig. 5). The two most discrepant gaps (area of 36.76 m<sup>2</sup> and 14.02 m<sup>2</sup> and mean height loss of 1.13 m and 2.13 m, respectively) were only detected in the field and without prior systematic classification.

290



295 **Figure 4: Size distribution of gaps formed in the INVENTA plot, Central Amazon, Brazil, over the period from 18<sup>th</sup> September 2018 to 19<sup>th</sup> January 2021. Gaps were measured from inventory plot surveys (red) and UAV imagery data (blue). Both data sets were fit using a Lognormal function (dotted lines).**



300 **Figure 5: Relationship between mean canopy height loss and gap area for gaps formed in the INVENTA plot, Central Amazon, Brazil, over the period from 18<sup>th</sup> September 2018 to 19<sup>th</sup> January 2021. Gap area was calculated from the UAV Imagery data. The x-axis is log-scaled.**

The size distribution of gaps larger than 9 m<sup>2</sup> (field data) and 10 m<sup>2</sup> (UAV data) was better described by the Lognormal function (Table S5, Fig. 4). For the distribution of gaps larger than 25 m<sup>2</sup> was better described by the Weibull and Power-law function in both methods (Table S5, Fig. S2b).

### 3.3 Mechanisms of gap formation and structure, and released biomass

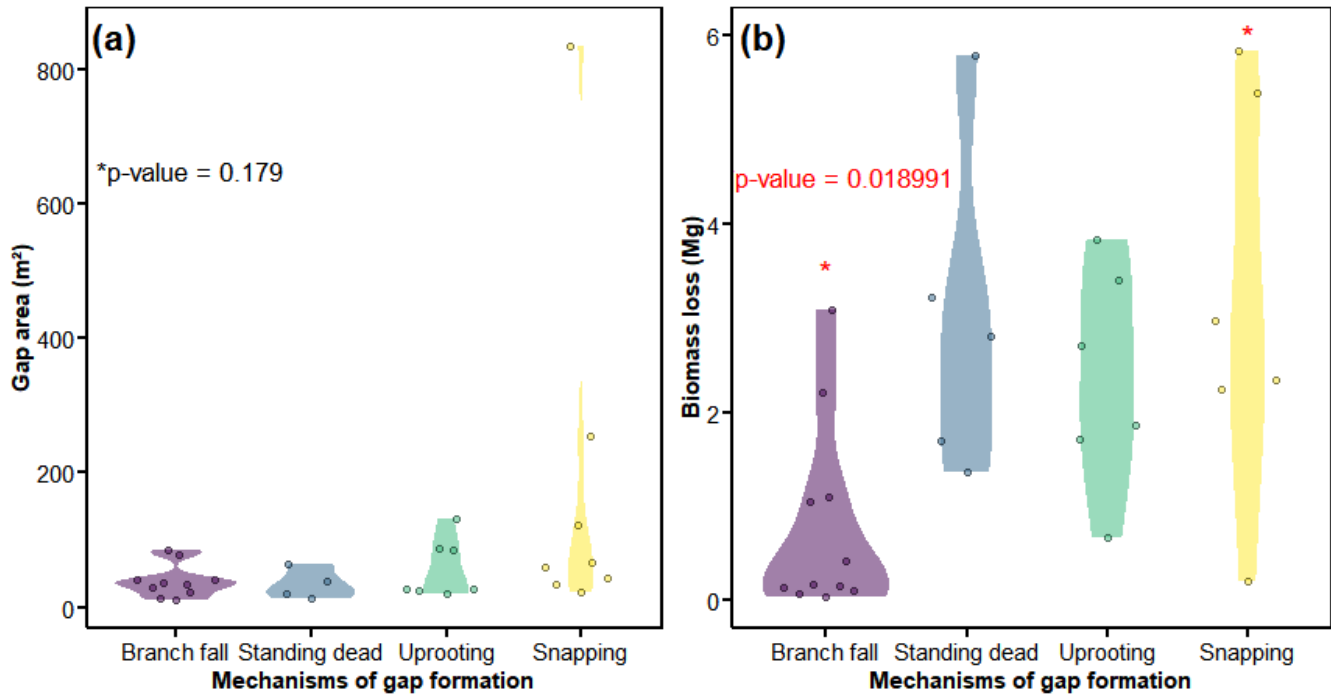
Branch fall was the most frequent mechanism of gap formation, accounting for 34.38 % (n= 11) of all detected gaps (Table 2). However, the total area accumulated by these gaps accounted for only 17.01 % of the total disturbed area. While gaps formed by tree snapping had the second highest frequency (n= 8 or 25 % of the total number of detected gaps) (Table 2), this mechanism accounted for 59.1 % of the total disturbed area. This result indicates that tree snapping was the most important mechanism of gap formation in respect to the overall disturbed area (Table 2). Uprooting and the fall of standing dead trees were the third and fourth most frequent mechanism of gap formation accounting for 16.53 % (n= 7) and 7.37 % (n= 6) of the total disturbed area, respectively (Table 2).

Branch fall, uprooting, snapping and standing dead trees accounted for the 52.9 %, 10 %, 6.7 % and 10 % of number of gaps detected on the imagery, respectively. For gaps only identified from field data, these mechanisms accounted for 60 %, 10.3 %, 6.9 % and 3.4 %, respectively.

We found no clear differences in the area attributed to gaps formed by branch fall and the described tree-mortality modes (p= 0.179) (Fig. 6a). However, we found strong evidence that the biomass released in gaps formed by tree snapping was higher than that associated with gaps formed by branch fall (p= 0.019) (Fig. 6b, Fig. S3). The overall loss of biomass in our studied gaps (1.35 Mg ha<sup>-1</sup> year<sup>-1</sup>) accounts for 0.88 % of the stocks in an old-growth forest contiguous to our plot (355.67 ± 34.53 Mg ha<sup>-1</sup> (mean ± standard deviation) (Amaral et al., 2019).

**Table 2.** Relative contribution of the different mechanisms of gap formation observed in the INVENTA plot, Central Amazon, Brazil, between September 2018 and January 2021.

	<b>Gaps (number)</b>	<b>Proportion of gaps (%)</b>	<b>Total area (m<sup>2</sup>)</b>	<b>Proportion of total area (% m<sup>2</sup>)</b>
<b>Branch fall</b>	11	34.38	414.57	17.01
<b>Snapped dead</b>	8	25.00	1440.58	59.10
<b>Uprooted dead</b>	7	21.88	402.90	16.53
<b>Standing dead</b>	6	18.75	179.55	7.37
	<b>32</b>		<b>2437.60</b>	

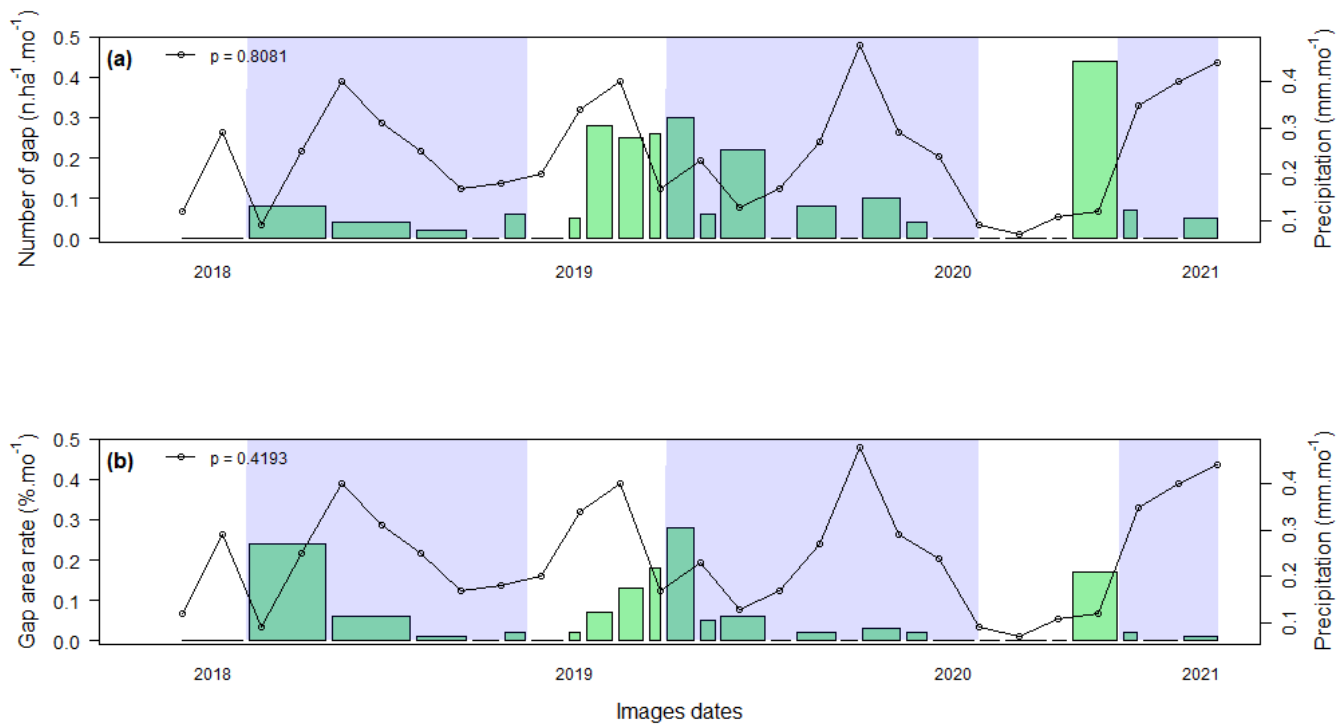


330 **Figure 6: Gap area (a) and biomass loss (b) for mechanisms of gap formation studied in the INVENTA plot, Central Amazon, Brazil, over the period from 18<sup>th</sup> September to 19<sup>th</sup> January 2021. The area of gaps was calculated from the UAV Imagery data. We detected significant differences in biomass loss only for branch fall and snapping (panel b).**

### 3.4 Rainfall seasonality and gap formation

335 The gap frequency and area rates were calculated using all 32 gaps identified during the studied period. Although gap frequency and area rate varied among the 28-month-period of monitoring, our data do not support that monthly rainfall influenced these metrics ( $p= 0.8081$  and  $p= 0.4193$ ; Fig. 7a and b, respectively). However, our data show that monthly gap-formation was marginally correlated with gap area rate for days with extreme rainfall events (i.e., above the 99<sup>th</sup> percentile,  $67.08 \text{ mm day}^{-1}$ ) ( $r= 0.37$  and  $p= 0.058$ ) (Fig. S4). The time interval accumulating the largest gap area (October 24, 2018 to December 27, 2018) included two extreme rainfall events:  $104 \text{ mm day}^{-1}$  on 20<sup>th</sup> October, and  $76 \text{ mm day}^{-1}$  on 8<sup>th</sup> November 2018 (Fig. S4).





340

**Figure 7: Seasonality of canopy gaps formed in INVENTA plot, Central Amazon, Brazil, during the period from 18<sup>th</sup> September to 19<sup>th</sup> January 2021. Gap frequency (a) and the cumulative rate of gap area formed over the observation period (expressed as % of the 18-ha study area per month) (b). The y2 axis (right) is the cumulative precipitation for each pair of time intervals between images (straight line with dots). The blue shading indicates the rainy season (September to June) for each year. The total area of each green rectangle is proportional to the total area of the gaps formed during the respective interval.**

345

## 4 Discussion

### 4.1 The mechanism of gap formation is related to the sensitivity of detection

We detected 17 and 16 gaps from field and imagery data, respectively; 14 gaps were identified from both methods. However, it is still possible that our approach underestimated the frequency of canopy disturbances smaller than the size threshold we analyzed (i.e., 5 m<sup>2</sup>). In a few cases, gaps detected from UAV imagery data (i.e., losses of canopy height) could not be detected from field surveys and did not fit the classical definition proposed by Brokaw (1982). While we found no evidences supporting strong divergences between the UAV and field data, this shall be tested beyond our study region and ideally with datasets

350

spanning larger spatial and temporal scales. These will likely contain a larger number of gaps, which allows for more detailed data analysis.

355 Gaps observed in the field but not captured on the imagery were relatively small and mainly formed by the fall of branches from live and standing dead trees. Nonetheless, branch fall of live and standing dead trees impacted relatively smaller areas. It is important to note that the mechanism of gap formation is related to the sensitivity of detection (Putz et al., 1983; Chao et al., 2009).

Our remote-sensing approach provides detailed data on the upper canopy of the forest, but no information on the understory.

360 Gaps were defined as disturbed patches with total area  $> 5 \text{ m}^2$  and with reductions of canopy height greater than 10 m. These thresholds were established based on the nominal resolution of our processed imagery (1 m) and the scale at which the forest inventories were conducted, i.e., tree level. Overall, the fall of branches and/or standing dead trees produced severe damage mostly in the upper canopy while the understory remained intact. Therefore, upper canopy gaps detected remotely were not always detected on the ground using the definition by Brokaw. This pattern shows that apart from covering relatively large  
365 areas at low costs, UAV photogrammetry is an efficient method for monitoring gap dynamics, with detailed information on upper canopy disturbance usually not visible from the forest ground.

We believe our approach combining field with remote sensing data provides interesting insights on concepts and methods for quantifying gaps and their effects on forest dynamics. Classical methods based on field observations are efficient to detect gaps extending from the upper canopy to the understory of the forest, and are crucial for validating remote tools, and for  
370 quantifying and modeling associated losses of biomass. High-resolution photogrammetry allows for more precise measurements of the features of the gaps, including those restricted to upper canopy and/or causing minor damage. Although more frequent, small-scale disturbances not implying tree mortality such as defoliation and branch fall are often neglected in forest inventories (Zuleta et al., 2023). Our study brings novel knowledge on the contribution of these events to ecosystem processes such as carbon cycle. Quantifying the size-distribution of gaps and their landscape importance is crucial to  
375 understand how forests respond to shifts in the disturbance regimes triggered by climate change and land use.

To our knowledge, this is the first study quantifying biomass losses associated with understory gaps. Here we demonstrated that these gaps contribute relatively little to landscape patterns of biomass. Still, future studies are required to address their importance to processes regulating patterns of species distribution and diversity. UAV photogrammetry has a relatively low cost, is simpler to process and thus can feasible be repeated in other regions of interest. Future studies may expand the existing  
380 knowledge on the size distribution and dynamics of gaps by combining sensors with different resolution. If combined with LiDAR, UAV imagery can be used to trace and quantify the regional importance of relatively smaller but more frequent events of tree mortality and damage not detectable with existing medium space-resolution satellite imagery.

## 385 4.2 There was no evidence for strong variation in the area between imagery and field data

Our tests comparing gaps detected from UAV photogrammetry and field data are rarely found in the literature (Yue et al., 2019), especially for dense tropical forest. Although understory gaps can be missed, the results of our research confirm the suitability and robustness of UAV photogrammetry for monitoring canopy dynamics in closed-canopy forests. When combined with continuous forest inventory, UAV photogrammetry at high temporal and spatial resolution can also reveal associated  
390 mechanisms of gap formation and released biomass.

However, the differences we found in perimeter and GSCI between imagery and field data indicate that the shape of gaps identified remotely and, in the field, can diverge. In our study, the differences between these methods are likely due to describing field-identified gaps as polygons that always had eight vertices. This contrasts with our remote estimates, on which losses of height ( $z$  value) and gap geometry were computed from  $1 \text{ m}^2$  pixels and for polygons which had a varying number of  
395 vertices. The shape of gaps measured in the field tended to be elliptical (Runkle, 1981) and triangular (Eysenrode et al., 1998). To date, most methods describing the shape and area of gaps focused on a two-dimensional projection of the canopy to the forest floor. In these two-dimensional assessments, there are three main assumptions: (i) most of the gaps have an uniform elliptical shape; (ii) the shape of irregular gaps can be approximated with several measurements; and (iii) the area of irregular-shaped gaps can be only be calculated from hemispherical photos (Schliemann and Bockheim, 2011). Here, we applied high-  
400 resolution imagery to assess gap geometry more detailed and beyond the number of vertices commonly applied in traditional field measurements. Vepakomma et al., (2008) combined LiDAR point cloud and field data from a boreal forest and also reported great differences in the shape of gaps derived from these two approaches. According to these authors, the more complex the shape and perimeter, the greater is the difference between the remote and field measurements (i.e., ground truth). Although the area of the gaps did not vary between our two methods, the reported variations in perimeter and GSCI revealed  
405 that imagery data allow for more complex shapes that can better represent natural disturbances (Lertzman and Krebs, 1991; Gagnon et al., 2004). This was true for our study region, for which gaps detected from imagery data had a greater variety of shapes, often irregular. The shape is an important feature for understanding the structure and dynamics of tropical forests (Jucker, 2022), which is important for determining microsite resource availability (Canham et al., 1994) from the center to edge of gaps (Gagnon et al., 2004). For the Amazon, there is still little research on how the shape of gaps varies across  
410 environmental and disturbance gradients (Malhi and Román-Cuesta, 2008).

The higher frequency of relatively small gaps we report here corroborates other studies that used different detection and classification methods (Lawton and Putz, 1988; Brokaw, 1982; Yavitt et al., 1995; Vepakomma et al., 2008; Asner et al., 2013; Leitold et al., 2018; Dalagnol et al., 2021; Gorgens et al., 2023). The Power law distribution had the steepest slope among the other tested functions. The distribution fit with remote data had a relative lower slope, i.e., of higher frequency of gaps larger  
415 than 100 m. This is the first study combining UAV and field data to assess the size distribution canopy gaps in terra-firme Amazon forests.

The frequency of gaps larger than 10 m<sup>2</sup> was better captured by a Lognormal function. This can be explained by the size threshold we use for defining our gaps. The relative lower density of small canopy disturbances compared to what would be expected under a power function may be partially explained by lower detection frequencies, i.e., measurement bias (Araujo et al., 2021). This may be more important for gaps < 10 m<sup>2</sup>. Still, our results show that independent of the detection method, the best fit describing the size frequency of gaps from 9 m<sup>2</sup> to 835 m<sup>2</sup> in our study region was achieved with Lognormal. As confirmed by our synchronized forest inventories, we believe that this pattern was not biased by gaps eventually not detected from imagery data. Furthermore, the lognormal distribution pattern was also observed for gap size distributions in various forest types with field monitoring of the size frequency distribution (Naka, 1982; Runkle, 1982; Spies et al., 1990; Yamamoto, 1998). This confirms the potential of UAV imagery for similar monitoring of the distribution of field data at the local scale. However, Lognormal function shows a trend of lower frequency in the smallest classes, followed by frequency, and reduces again as the size of the gaps increases. For the field data, the first point on the graph is smaller than the second, fitting perfectly for the Lognormal function. For the UAV image data, on the other hand, the second point is larger than the third point on the graph, and we believe this is why the lognormal did not fit. In this case, the Weibull fit is more flexible for this small variation of size frequency distribution.

### **4.3 Small-scale disturbances dominate canopy dynamics and associated biomass losses in Central Amazon**

Repeated and field measurements provide allow for quantifying the relative importance of mechanisms of gap formation in Amazon forests. Our results resemble a previous study using repeated high-density Lidar data on another location in Central Amazon, Santarém, Pará (Leitold et al., 2018). These authors showed that biomass losses due to single and multiple events of branch fall events accounted for only 20% of the total estimated biomass loss from canopy and understory trees. In Panama, branch fall accounted for 43.5% of the gap density over a period of five years, but only for 23% of the total disturbed area (Araujo et al., 2021). Like in our study region, this pattern highlights that the size and shape of gaps is largely influenced by modes of tree mortality. In tropical forests, the mortality rate of trees from 1 cm to 10 cm DBH was unrelated to tree biomass losses among trees >10 cm DBH (Gora and Esquivel-Muelbert, 2021). Still, there is a relative contribution of different tree mortality factors across a continuum of tree sizes. Zuleta et al. 2022 showed that uprooted trees have significantly larger size (i.e., DBH). However, snapping was a more frequent mode of tree mortality compared with standing dead or uprooting. Although of less importance among large trees, falling branches can affect small trees differently and promote changes or filter out saplings of canopy and also understory species.

Crown damage and/or loss is one of the most impactful risky aspects leading to tree mortality (Zuleta et al., 2022). Almost half of the aboveground biomass of tropical forests (42%, range of 12% – 76% across forests) is lost due to damage to live trees (Zuleta et al., 2023). If climate change results in a higher frequency of storms and extreme winds, branch fall and tree mortality rates can also be expected to increase. This may affect carbon stocks and dynamics, as well as the functional composition of these forests at the landscape level (Magnabosco Marra et al., 2018; Denslow et al., 1998).

#### 4.4 Extreme rainfall-events control gap formation

450 In our study site, the gap area and frequency rates varied over time. The gaps formed during a single period of less than a month (21<sup>st</sup> October to 1<sup>st</sup> November 2020) accounted for 20.4 % of the total disturbed area. Still, we did not find a correlation between gap area and frequency rates with the accumulated precipitation over time. Fontes et al. (2018) reported a strong positive correlation ( $r= 0.85$ ) of cumulative precipitation and tree mortality over a 1-year period on a plot contiguous to our study site, which may be related to interannual variability of the rainfall (Marengo et al., 2009). Nonetheless, we found a  
455 positive correlation between gap area rate and the frequency of extreme rainfall events. As in our study site, the frequency of rainfall events above the 98<sup>th</sup> percentile (24.3 mm hour<sup>1</sup>) explained a large fraction of the variation in rates of gap area over measurement intervals ( $r = 0.46$ ) for a tropical forest in Panama (Araujo et al., 2021). We also understand that a comprehensive assessment of the influence of precipitation on gap formation requires longer-term data addressing seasonal and interannual variability.

460 As recently reported for the Amazon, areas with stronger winds and more frequent lightning have larger gaps (Reis et al., 2021). Extreme winds and rain can cause extensive damage (single gaps >10 ha) in the forest (Negrón-Juárez et al., 2018; Espírito-Santo et al., 2014; Magnabosco Marra et al., 2014b), but the size distribution and landscape effects of small-scale storm-related disturbances are more challenging to study. Convective rainfall and extreme wind gusts promote crown damage, snapping and uprooting from individual to large clusters of trees (Magnabosco Marra et al. 2014b; Negrón-Juárez et al. 2011;  
465 Nelson et al. 1994). The vulnerability of trees to extreme wind and rainfall vary across Amazon regions (Negrón-Juárez et al., 2018; Urquiza Muñoz et al., 2021). Thus, projected shifts on the intensity and frequency of these events can also be expected to have particular effects on current patterns of tree mortality and biomass.

In addition to seasonal patterns of rainfall and wind, gap formation is also affected by local topography and soil (De Toledo et al., 2011). In Central Amazon forests, despite little variation associated directly with soil and slope, tree mortality due to  
470 uprooting and snapping can increase with more frequent storms (De Toledo et al., 2012). As climate change is expected to alter the frequency and intensity of tropical storms, soil attributes and topography may become more useful to improve estimates of tree mortality and biomass losses over large areas in Amazonia.

#### 5 Conclusion

By combining high temporal and spatial resolution UAV imagery with field data we could reliably assess landscape patterns  
475 of gaps and associated losses of biomass for a closed-canopy Amazon forest. Mechanisms of gap formation could only be distinguished in the field. Tree snapping was associated with the higher losses of biomass. Although with relatively lower losses of biomass, branchfall was the most frequent mechanism of gap formation. This finding highlights the importance of merging field and remote sensing data for assessing landscape processes regulating carbon cycle. Future studies could advance current knowledge by generating proxies for distinguishing mechanisms of gap formation using RGB UAV imagery.

## 480 **6 Acknowledgments**

This study is part of the Wind–Tree Interaction Project (INVENTA) and the Amazon Tall Tower Observatory (ATTO), funded by the German Federal Ministry of Education and Research (BMBF, contracts 01LB1001A and 01LK1602A), the Brazilian Ministry of Science, Technology and Innovation (MCTI/FINEP, contract 01.11.01248.00) and the Max Planck Society (MPG). ATTO is also supported by the Fundação de Amparo à Pesquisa do Estado do Amazonas (FAPEAM), Fundação de Amparo à  
485 Pesquisa do Estado de São Paulo (FAPESP), Universidade do Estado do Amazonas (UEA), Instituto Nacional de Pesquisas Amazônia (INPA), Programa de Grande Escala da Biosfera-Atmosfera na Amazônia (LBA) and the SDS/CEUC/RDS-Uatumã. Our study site is also supported by the INCT Madeiras da Amazônia. We thank the Forest Management Laboratory of the National Institute for Amazonian Research (LMF/INPA) for logistic support.

### **Author contributions**

490 AS and DMM planned and designed the research; AS, RFA and CHSC collected drone data; AS, RFA, CHSC and FRSS processed drone imagery; AS and FRSS collected field data; AS, DMM, RFA and CHSC analyzed the data; AS and DMM wrote the manuscript with the support from all authors.

### **Competing interests**

The authors declare that they have no conflict of interest.

## 495 **References**

- Aleixo, I., Norris, D., Hemerik, L., Barbosa, A., Prata, E., Costa, F., and Poorter, L.: Amazonian rainforest tree mortality driven by climate and functional traits, *Nat. Clim. Chang.*, 9, 384–388, <https://doi.org/10.1038/s41558-019-0458-0>, 2019.
- Allen, C. D., Breshears, D. D., and McDowell, N. G.: On underestimation of global vulnerability to tree mortality and forest die-off from hotter drought in the Anthropocene, *Ecosphere*, 6, 1–55, <https://doi.org/10.1890/ES15-00203.1>, 2015.
- 500 Amaral, M., Lima, A., Higuchi, F., dos Santos, J., and Higuchi, N.: Dynamics of Tropical Forest Twenty-Five Years after Experimental Logging in Central Amazon Mature Forest, *Forests*, 10, 89, <https://doi.org/10.3390/f10020089>, 2019.
- Araujo, R. F.: Estrutura do dossel, dinâmica florestal e fenologia foliar com uso de Aeronave Remotamente Pilotada na Amazônia central, Ph.D. thesis, Instituto Nacional de Pesquisas da Amazônia, 80 pp., 2019.
- Araujo, R. F., Nelson, B. W., Celes, C. H. S., and Chambers, J. Q.: Regional distribution of large blowdown patches across  
505 Amazonia in 2005 caused by a single convective squall line, *Geophys. Res. Lett.*, 44, 7793–7798, <https://doi.org/10.1002/2017GL073564>, 2017.
- Araujo, R. F., Chambers, J. Q., Celes, C. H. S., Muller-Landau, H. C., dos Santos, A. P. F., Emmert, F., Ribeiro, G. H. P. M.,

- Gimenez, B. O., Lima, A. J. N., Campos, M. A. A., and Higuchi, N.: Integrating high resolution drone imagery and forest inventory to distinguish canopy and understory trees and quantify their contributions to forest structure and dynamics, *PLoS One*, 15, 1–16, <https://doi.org/10.1371/journal.pone.0243079>, 2020.
- 510 Araujo, R. F., Grubinger, S., Celes, C. H. S., Negrón-Juárez, R. I., Garcia, M., Dandois, J. P., and Muller-Landau, H. C.: Strong temporal variation in treefall and branchfall rates in a tropical forest is related to extreme rainfall: Results from 5 years of monthly drone data for a 50 ha plot, *Biogeosciences*, 18, 6517–6531, <https://doi.org/10.5194/bg-18-6517-2021>, 2021.
- Araujo, R. F., Celes, C. H. S., Negrón-Juárez, R. I., and Muller-Landau, H. C.: Analysis codes and datasets: Strong temporal  
515 variation in treefall and branchfall rates in a tropical forest is related to extreme rainfall: results from five years of monthly drone data for a 50-ha plot, *Zenodo [code]*, <https://doi.org/10.5281/zenodo.5786740>, 2021a.
- Asner, G. P., Kellner, J. R., Kennedy-Bowdoin, T., Knapp, D. E., Anderson, C., and Martin, R. E.: Forest Canopy Gap Distributions in the Southern Peruvian Amazon, *PLoS One*, 8, e60875, <https://doi.org/10.1371/journal.pone.0060875>, 2013.
- Baker, T. R., Phillips, O. L., Malhi, Y., Almeida, S., Arroyo, L., Di Fiore, A., Erwin, T., Higuchi, N., Killeen, T. J., Laurance,  
520 S. G., Laurance, W. F., Lewis, S. L., Monteagudo, A., Neill, D. A., Núñez Vargas, P., Pitman, N. C. A., Silva, J. N. M., and Vásquez Martínez, R.: Increasing biomass in Amazonian forest plots, *Philos. Trans. R. Soc. B Biol. Sci.*, 359, 353–365, <https://doi.org/10.1098/rstb.2003.1422>, 2004.
- Brienen, R. J. W., Phillips, O. L., Feldpausch, T. R., Gloor, E., Baker, T. R., Lloyd, J., Lopez Gonzalez, G., Monteagudo  
Mendoza, A., Malhi, Y., Lewis, S. L., and Vásquez, R.: Long-term decline of the Amazon carbon sink, *Nature*, 519, 344–348,  
525 <https://doi.org/10.1038/nature14283>, 2015.
- Brokaw, N. V. L.: The Definition of Treefall Gap and Its Effect on Measures of Forest Dynamics, *Biotropica*, 14, 158, <https://doi.org/10.2307/2387750>, 1982.
- Burnham, K. P. and Anderson, D. R.: *Multimodel inference: A Practical Information-Theoretic Approach*, 488 pp., 2002.
- Canham, C. D., Finzi, A. C., Pacala, S. W., and Burbank, D. H.: Causes and consequences of resource heterogeneity in forests:  
530 interspecific variation in light transmission by canopy trees, *Can. J. For. Res.*, 24, 337–349, <https://doi.org/10.1139/x94-046>, 1994.
- Carvalho, L.: An Improved Evaluation of Kolmogorov’s Distribution, *J. Stat. Softw.*, 65, 1–3, <https://doi.org/10.18637/jss.v065.c03>, 2015.
- Chambers, J. Q., Negrón-Juarez, R. I., Marra, D. M., Di Vittorio, A., Tews, J., Roberts, D., Ribeiro, G. H. P. M., Trumbore,  
535 S. E., and Higuchi, N.: The steady-state mosaic of disturbance and succession across an old-growth central Amazon forest landscape, *Proc. Natl. Acad. Sci. U. S. A.*, 110, 3949–3954, <https://doi.org/10.1073/pnas.1202894110>, 2013.
- Chao, K. J., Phillips, O. L., Monteagudo, A., Torres-Lezama, A., and Vásquez Martínez, R.: How do trees die? Mode of death in northern Amazonia, *J. Veg. Sci.*, 20, 260–268, <https://doi.org/10.1111/j.1654-1103.2009.05755.x>, 2009.
- Clark, D. A., Asao, S., Fisher, R., Reed, S., Reich, P. B., Ryan, M. G., Wood, T. E., and Yang, X.: Reviews and syntheses:  
540 Field data to benchmark the carbon cycle models for tropical forests, *Biogeosciences*, 14, 4663–4690, <https://doi.org/10.5194/bg-14-4663-2017>, 2017.



- Cushman, K. C., Detto, M., García, M., and Muller-Landau, H. C.: Soils and topography control natural disturbance rates and thereby forest structure in a lowland tropical landscape, *Ecol. Lett.*, 25, 1126–1138, <https://doi.org/10.1111/ele.13978>, 2022.
- Dalagnol, R., Wagner, F. H., Galvão, L. S., Streher, A. S., Phillips, O. L., Gloor, E., Pugh, T. A. M., Ometto, J. P. H. B., and  
545 Aragão, L. E. O. C.: Large-scale variations in the dynamics of Amazon forest canopy gaps from airborne lidar data and opportunities for tree mortality estimates, *Sci. Rep.*, 11, 1388, <https://doi.org/10.1038/s41598-020-80809-w>, 2021.
- Denslow, J. S.: Gap Partitioning among Tropical Rainforest Trees, *Biotropica*, 12, 47, <https://doi.org/10.2307/2388156>, 1980.
- Denslow, J. S.: Tropical Rainforest gaps and tree species diversity, *Annu. Rev. Ecol. Evol. Syst.*, 18, 431–51, 1987.
- Denslow, J. S., Ellison, A. M., and Sanford, R. E.: Treefall gap size effects on above- and below-ground processes in a tropical  
550 wet forest, *J. Ecol.*, 86, 597–609, <https://doi.org/10.1046/j.1365-2745.1998.00295.x>, 1998.
- Espírito-Santo, F. D. B., Gloor, M., Keller, M., Malhi, Y., Saatchi, S., Nelson, B., Junior, R. C. O., Pereira, C., Lloyd, J., Frolking, S., Palace, M., Shimabukuro, Y. E., Duarte, V., Mendoza, A. M., López-González, G., Baker, T. R., Feldpausch, T. R., Brien, R. J. W., Asner, G. P., Boyd, D. S., and Phillips, O. L.: Size and frequency of natural forest disturbances and the Amazon forest carbon balance, *Nat. Commun.*, 5, 1–6, <https://doi.org/10.1038/ncomms4434>, 2014.
- 555 Esquivel-Muelbert, A., Phillips, O. L., Brien, R. J. W., Fauset, S., Sullivan, M. J. P., Baker, T. R., Chao, K. J., Feldpausch, T. R., Gloor, E., Higuchi, N., Houwing-Duistermaat, J., Lloyd, J., Liu, H., Malhi, Y., Marimon, B., Marimon Junior, B. H., Monteagudo-Mendoza, A., Poorter, L., Silveira, M., Torre, E. V., Dávila, E. A., del Aguila Pasquel, J., Almeida, E., Loayza, P. A., Andrade, A., Aragão, L. E. O. C., Araujo-Murakami, A., Arets, E., Arroyo, L., Aymard C, G. A., Baisie, M., Baraloto, C., Camargo, P. B., Barroso, J., Blanc, L., Bonal, D., Bongers, F., Boot, R., Brown, F., Burban, B., Camargo, J. L., Castro,  
560 W., Moscoso, V. C., Chave, J., Comiskey, J., Valverde, F. C., da Costa, A. L., Cardozo, N. D., Di Fiore, A., Dourdain, A., Erwin, T., Llampazo, G. F., Vieira, I. C. G., Herrera, R., Honorio Coronado, E., Huamantupa-Chuquimaco, I., Jimenez-Rojas, E., Killeen, T., Laurance, S., Laurance, W., Levesley, A., Lewis, S. L., Ladvoat, K. L. L. M., Lopez-Gonzalez, G., Lovejoy, T., Meir, P., Mendoza, C., Morandi, P., Neill, D., Nogueira Lima, A. J., Vargas, P. N., de Oliveira, E. A., Camacho, N. P., Pardo, G., Peacock, J., Peña-Claros, M., Peñuela-Mora, M. C., Pickavance, G., Pipoly, J., Pitman, N., Prieto, A., Pugh, T. A.  
565 M., Quesada, C., Ramirez-Angulo, H., de Almeida Reis, S. M., Rejou-Machain, M., Correa, Z. R., Bayona, L. R., Rudas, A., Salomão, R., Serrano, J., Espejo, J. S., Silva, N., Singh, J., Stahl, C., Stropp, J., Swamy, V., Talbot, J., ter Steege, H., et al.: Tree mode of death and mortality risk factors across Amazon forests, *Nat. Commun.*, 11, <https://doi.org/10.1038/s41467-020-18996-3>, 2020.
- Eysenrode, D. S., Bogaert, J., Hecke, P. Van, and Impens, I.: Influence of tree-fall orientation on canopy gap shape in an  
570 Ecuadorian rain forest, *J. Trop. Ecol.*, 14, 865–869, <https://doi.org/10.1017/S0266467498000625>, 1998.
- Feng, Y., Negrón-Juárez, R. I., Romps, D. M., and Chambers, J. Q.: Amazon windthrow disturbances are likely to increase with storm frequency under global warming, *Nat. Commun.*, 14, 101, <https://doi.org/10.1038/s41467-022-35570-1>, 2023.
- Fontes, C. G., Chambers, J. Q., and Higuchi, N.: Revealing the causes and temporal distribution of tree mortality in Central Amazonia, *For. Ecol. Manage.*, 424, 177–183, <https://doi.org/10.1016/j.foreco.2018.05.002>, 2018.
- 575 Frelich, L.: Forest dynamics, *F1000Research*, 5, 183, <https://doi.org/10.12688/f1000research.7412.1>, 2016.

- Frolking, S., Palace, M. W., Clark, D. B., Chambers, J. Q., Shugart, H. H., and Hurtt, G. C.: Forest disturbance and recovery: A general review in the context of spaceborne remote sensing of impacts on aboveground biomass and canopy structure, *J. Geophys. Res. Biogeosciences*, 114, <https://doi.org/10.1029/2008JG000911>, 2009.
- 580 Gagnon, J. L., Jokela, E. J., Moser, W. ., and Huber, D. A.: Characteristics of gaps and natural regeneration in mature longleaf pine flatwoods ecosystems, *For. Ecol. Manage.*, 187, 373–380, <https://doi.org/10.1016/j.foreco.2003.07.002>, 2004.
- Getzin, S., Nuske, R. S., and Wiegand, K.: Using Unmanned Aerial Vehicles (UAV) to Quantify Spatial Gap Patterns in Forests, 6988–7004, <https://doi.org/10.3390/rs6086988>, 2014.
- Gimenez, B. O., dos Santos, L. T., Gebara, J., Celes, C. H. S., Durgante, F. M., Lima, A. J. N., Santos, J. dos, and Higuchi, N.: Tree climbing techniques and volume equations for *Eschweilera* (Matá-Matá), a hyperdominant genus in the Amazon  
585 Forest, *Forests*, 8, <https://doi.org/10.3390/f8050154>, 2017.
- Gloor, M., Brienen, R. J. W., Galbraith, D., Feldpausch, T. R., Schöngart, J., Guyot, J. L., Espinoza, J. C., Lloyd, J., and Phillips, O. L.: Intensification of the Amazon hydrological cycle over the last two decades, *Geophys. Res. Lett.*, 40, 1729–1733, <https://doi.org/10.1002/grl.50377>, 2013.
- Gora, E. M. and Esquivel-Muelbert, A.: Implications of size-dependent tree mortality for tropical forest carbon dynamics, *Nat.*  
590 *Plants*, 7, 384–391, <https://doi.org/10.1038/s41477-021-00879-0>, 2021.
- Gorgens, E. B., Keller, M., Jackson, T., Marra, D. M., Reis, C. R., de Almeida, D. R. A., Coomes, D., and Ometto, J. P.: Out of steady state: Tracking canopy gap dynamics across Brazilian Amazon, *Biotropica*, 1–12, <https://doi.org/10.1111/btp.13226>, 2023.
- Grubb, P. J.: the Maintenance of Species-Richness in Plant Communities: the Importance of the Regeneration Niche, *Biol. Rev.*, 52, 107–145, <https://doi.org/10.1111/j.1469-185x.1977.tb01347.x>, 1977.
- Hubbell, S. P., Foster, R. B., O’Brien, S. T., Harms, K. E., Condit, R., Wechsler, B., Wright, S. J., and de Lao, S. L.: Light-Gap Disturbances, Recruitment Limitation, and Tree Diversity in a Neotropical Forest, *Science* (80-. ), 283, 554–557, <https://doi.org/10.1126/science.283.5401.554>, 1999.
- Iglhaut, J., Cabo, C., Puliti, S., Piermattei, L., O’Connor, J., and Rosette, J.: Structure from Motion Photogrammetry in  
600 Forestry: a Review, *Curr. For. Reports*, 5, 155–168, <https://doi.org/10.1007/s40725-019-00094-3>, 2019.
- IPCC: Summary for Policymakers., edited by: Masson-Delmotte, V., P.Zhai, Pirani, A., Connors, S. L., Péan, C., Berger, S., Caud, N., Chen, Y., Goldfarb, L., Gomis, M. I., Huang, M., Leitzell, K., Lonnoy, E., Matthews, J. B. R., Maycock, T. K., Waterfield, T., Yelekçi, O., Yu, R., and Zhou, B., In Press., 40 pp., 2021.
- Jucker, T.: Deciphering the fingerprint of disturbance on the three-dimensional structure of the world’s forests, *New Phytol.*,  
605 233, 612–617, <https://doi.org/10.1111/nph.17729>, 2022.
- Kellner, J. R. and Asner, G. P.: Winners and losers in the competition for space in tropical forest canopies, *Ecol. Lett.*, 17, 556–562, <https://doi.org/10.1111/ele.12256>, 2014.
- Kellner, J. R., Clark, D. B., and Hubbell, S. P.: Pervasive canopy dynamics produce short-term stability in a tropical rain forest landscape, *Ecol. Lett.*, 12, 155–164, <https://doi.org/10.1111/j.1461-0248.2008.01274.x>, 2009.

- 610 Laurance, W. F., Oliveira, A. A., Laurance, S. G., Condit, R., Nascimento, H. E. M., Sanchez-Thorin, A. C., Lovejoy, T. E., Andrade, A., D'Angelo, S., Ribeiro, J. E., and Dick, C. W.: Pervasive alteration of tree communities in undisturbed Amazonian forests, *Nature*, 428, 171–175, <https://doi.org/10.1038/nature02383>, 2004.
- Lawton, R. O. and Putz, F. E.: Natural Disturbance and Gap-Phase Regeneration in a Wind-Exposed Tropical Cloud Forest, *Ecology*, 69, 764–777, <https://doi.org/10.2307/1941025>, 1988.
- 615 Leitold, V., Morton, D. C., Longo, M., Dos-Santos, M. N., Keller, M., and Scaranello, M.: El Niño drought increased canopy turnover in Amazon forests, *New Phytol.*, 219, 959–971, <https://doi.org/10.1111/nph.15110>, 2018.
- Lertzman, K. P. and Krebs, C. J.: Gap-phase structure of a subalpine old-growth forest, *Can. J. For. Res.*, 21, 1730–1741, <https://doi.org/10.1139/x91-239>, 1991.
- Lima, A. J. N., Suwa, R., De Mello Ribeiro, G. H. P., Kajimoto, T., Dos Santos, J., Da Silva, R. P., De Souza, C. A. S., De  
620 Barros, P. C., Noguchi, H., Ishizuka, M., and Higuchi, N.: Allometric models for estimating above- and below-ground biomass in Amazonian forests at São Gabriel da Cachoeira in the upper Rio Negro, Brazil, *For. Ecol. Manage.*, 277, 163–172, <https://doi.org/10.1016/j.foreco.2012.04.028>, 2012.
- Magnabosco Marra, D., Chambers, J. Q., Higuchi, N., Trumbore, S. E., Ribeiro, G. H. P. M., Dos Santos, J., Negrón-Juárez, R. I., Reu, B., and Wirth, C.: Large-scale wind disturbances promote tree diversity in a Central Amazon forest, *PLoS One*, 9,  
625 <https://doi.org/10.1371/journal.pone.0103711>, 2014.
- Magnabosco Marra, D., Pereira B.A.S., Fagg C.W., Felfili J.M.: Trees and environmental variables influence the natural regeneration of seasonally dry tropical forest in Central Brazil, *Neotropical Biology and Conservation*, 9(2), 62-77, <https://doi.org/10.4013/nbc.2014.92.01>, 2014a.
- Magnabosco Marra, D., Chambers, J. Q., Higuchi, N., Trumbore, S. E., Ribeiro, G. H. P. M., Dos Santos, J., Negrón-Juárez,  
630 R. I., Reu, B., and Wirth, C.: Large-scale wind disturbances promote tree diversity in a Central Amazon forest, *PLoS One*, 9, <https://doi.org/10.1371/journal.pone.0103711>, 2014b.
- Magnabosco Marra, D., Trumbore, S. E., Higuchi, N., Ribeiro, G. H. P. M., Negrón-Juárez, R. I., Holzwarth, F., Rifai, S. W., dos Santos, J., Lima, A. J. N., Kinupp, V. F., Chambers, J. Q., and Wirth, C.: Windthrows control biomass patterns and functional composition of Amazon forests, *Glob. Chang. Biol.*, 24, 5867–5881, <https://doi.org/10.1111/gcb.14457>, 2018.
- 635 Malhi, Y. and Román-Cuesta, R. M.: Analysis of lacunarity and scales of spatial homogeneity in IKONOS images of Amazonian tropical forest canopies, *Remote Sens. Environ.*, 112, 2074–2087, <https://doi.org/10.1016/j.rse.2008.01.009>, 2008.
- Marengo, J. A., Jones, R., Alves, L. M., and Valverde, M. C.: Future change of temperature and precipitation extremes in South America as derived from the PRECIS regional climate modeling system, *Int. J. Climatol.*, 29, 2241–2255, <https://doi.org/10.1002/joc.1863>, 2009.
- 640 McDowell, N., Allen, C. D., Anderson-Teixeira, K., Brando, P., Brienen, R., Chambers, J., Christoffersen, B., Davies, S., Doughty, C., Duque, A., Espirito-Santo, F., Fisher, R., Fontes, C. G., Galbraith, D., Goodsman, D., Grossiord, C., Hartmann, H., Holm, J., Johnson, D. J., Kassim, A. R., Keller, M., Koven, C., Kueppers, L., Kumagai, T., Malhi, Y., McMahon, S. M., Mencuccini, M., Meir, P., Moorcroft, P., Muller-Landau, H. C., Phillips, O. L., Powell, T., Sierra, C. A., Sperry, J., Warren,

- J., Xu, C., and Xu, X.: Drivers and mechanisms of tree mortality in moist tropical forests, *New Phytol.*, 219, 851–869, <https://doi.org/10.1111/nph.15027>, 2018.
- 645 Negrón-Juárez, R., Magnabosco-Marra, D., Feng, Y., Urquiza-Muñoz, J. D., Riley, W. J., and Chambers, J. Q.: Windthrow characteristics and their regional association with rainfall, soil, and surface elevation in the Amazon, *Environ. Res. Lett.*, 18, 014030, <https://doi.org/10.1088/1748-9326/acaf10>, 2023.
- Negrón-Juárez, R. I., Chambers, J. Q., Guimaraes, G., Zeng, H., Raupp, C. F. M., Marra, D. M., Ribeiro, G. H. P. M., Saatchi, 650 S. S., Nelson, B. W., and Higuchi, N.: Widespread Amazon forest tree mortality from a single cross-basin squall line event, *Geophys. Res. Lett.*, 37, 1–5, <https://doi.org/10.1029/2010GL043733>, 2010.
- Negrón-Juárez, R. I., Chambers, J. Q., Marra, D. M., Ribeiro, G. H. P. M., Rifai, S. W., Higuchi, N., and Roberts, D.: Detection of subpixel treefall gaps with Landsat imagery in Central Amazon forests, *Remote Sens. Environ.*, 115, 3322–3328, <https://doi.org/10.1016/j.rse.2011.07.015>, 2011.
- 655 Negrón-Juárez, R. I., Jenkins, H. S., Raupp, C. F. M., Riley, W. J., Kueppers, L. M., Marra, D. M., Ribeiro, G. H. P. M., Monteiro, M. T. F., Candido, L. A., Chambers, J. Q., and Higuchi, N.: Windthrow variability in central Amazonia, *Atmosphere (Basel)*, 8, 1–17, <https://doi.org/10.3390/atmos8020028>, 2017.
- Negrón-Juárez, R. I., Holm, J. A., Marra, D. M., Rifai, S. W., Riley, W. J., Chambers, J. Q., Koven, C. D., Knox, R. G., McGroddy, M. E., Di Vittorio, A. V., Urquiza-Muñoz, J., Tello-Espinoza, R., Muñoz, W. A., Ribeiro, G. H. P. M., and Higuchi, 660 N.: Vulnerability of Amazon forests to storm-driven tree mortality, *Environ. Res. Lett.*, 13, <https://doi.org/10.1088/1748-9326/aabe9f>, 2018.
- Nelson, B. W., Kapos, V., Adams, J. B., Oliveira, W. J., and Braun, O. P. G.: Forest Disturbance by Large Blowdowns in the Brazilian Amazon, *Ecology*, 75, 853–858, <https://doi.org/10.2307/1941742>, 1994.
- Oliveira, A. A. D. E. and Mori, S. A.: A central Amazonian terra firme forest. I. High tree species richness on poor soils, 665 *Biodivers. Conserv.*, 8, 1219–1244, <https://doi.org/doi.org/10.1023/A:1008908615271>, 1999.
- Ometto, J. P., Gorgens, B. G., Assis, M., Cantinho, R. Z., Pereira, F. R. de S., and Sato, L. Y.: L3A - Airborne LiDAR transects summary collected by EBA in the Brazilian Amazon, [data set], <https://doi.org/https://zenodo.org/record/4968706>, 2021.
- Pan, Y., Birdsey, R. A., Phillips, O. L., and Jackson, R. B.: The structure, distribution, and biomass of the world's forests, *Annu. Rev. Ecol. Evol. Syst.*, 44, 593–622, <https://doi.org/10.1146/annurev-ecolsys-110512-135914>, 2013.
- 670 Phillips, O. L. and Gentry, A. H.: Increasing Turnover Through Time in Tropical Forests, *Science (80-. )*, 263, 954–958, <https://doi.org/10.1126/science.263.5149.954>, 1994.
- Putz, F. E., Coley, P. D., Lu, K., Montalvo, A., and Aiello, A.: Uprooting and snapping of trees: structural determinants and ecological consequences, *Can. J. For. Res.*, 13, 1011–1020, <https://doi.org/10.1139/x83-133>, 1983.
- Reis, C. R., Jackson, T. D., Bastos Gorgens, E., Dalagnol, R., Jucker, T., Henrique Nunes, M., and Pierre Ometto, J.: Forest 675 structure and degradation drive canopy gap sizes across the Brazilian Amazon, *bioRxiv*, 2021.05.03.442416, <https://doi.org/https://doi.org/10.1101/2021.05.03.442416>, 2021.
- Ribeiro, G. H. P. M., Chambers, J. Q., Peterson, C. J., Trumbore, S. E., Marra, D. M., Wirth, C., Cannon, J. B., Négron-juárez,

- R. I., Lima, A. J. N., Paula, E. V. C. M. De, Santos, J., and Higuchi, N.: Forest Ecology and Management Mechanical vulnerability and resistance to snapping and uprooting for Central Amazon tree species, *For. Ecol. Manage.*, 380, 1–10, 680 <https://doi.org/10.1016/j.foreco.2016.08.039>, 2016.
- Runkle, J. R.: Gap Regeneration in Some Old-growth Forests of the Eastern United States, *Ecology*, 62, 1041–1051, <https://doi.org/10.2307/1937003>, 1981.
- Runkle, J. R. and Yetter, T. C.: Treefalls Revisited: Gap Dynamics in the Southern Appalachians, *Ecology*, 68, 417–424, <https://doi.org/10.2307/1939273>, 1987.
- 685 Santos, L. T., Marra, D. M., Trumbore, S., Camargo, P. B. De, Lima, A. J. N. N., Ribeiro, G. H. P. M. P. M., Santos, J., Higuchi, N., Dos Santos, L. T., Marra, D. M., Trumbore, S., De Camargo, P. B., Negrón-Juárez, R. I., Lima, A. J. N. N., Ribeiro, G. H. P. M. P. M., Dos Santos, J., and Higuchi, N.: Windthrows increase soil carbon stocks in a central Amazon forest, *Biogeosciences*, 13, 1299–1308, <https://doi.org/10.5194/bg-13-1299-2016>, 2016.
- Schliemann, S. A. and Bockheim, J. G.: Methods for studying treefall gaps: A review, *For. Ecol. Manage.*, 261, 1143–1151, 690 <https://doi.org/10.1016/j.foreco.2011.01.011>, 2011.
- Senf, C.: Seeing the system from above – The use and potential of remote sensing for studying ecosystem dynamics (in press), *Ecosystems*, <https://doi.org/10.1007/s10021-022-00777-2>, 2022.
- Sombroek, W.: Spatial and Temporal Patterns of Amazon Rainfall, *AMBIO A J. Hum. Environ.*, 30, 388–396, <https://doi.org/10.1579/0044-7447-30.7.388>, 2001.
- 695 Tan, J., Jakob, C., Rossow, W. B., and Tselioudis, G.: Increases in tropical rainfall driven by changes in frequency of organized deep convection, *Nature*, 519, 451–454, <https://doi.org/10.1038/nature14339>, 2015.
- De Toledo, J. J., Magnusson, W. E., Castilho, C. V., and Nascimento, H. E. M.: How much variation in tree mortality is predicted by soil and topography in Central Amazonia?, *For. Ecol. Manage.*, 262, 331–338, <https://doi.org/10.1016/j.foreco.2011.03.039>, 2011.
- 700 De Toledo, J. J., Magnusson, W. E., Castilho, C. V., and Nascimento, H. E. M.: Tree mode of death in Central Amazonia: Effects of soil and topography on tree mortality associated with storm disturbances, *For. Ecol. Manage.*, 263, 253–261, <https://doi.org/10.1016/j.foreco.2011.09.017>, 2012.
- Urquiza Muñoz, J. D., Magnabosco Marra, D., Negrón-Juarez, R. I., Tello-Espinoza, R., Alegría-Muñoz, W., Pacheco-Gómez, T., Rifai, S. W., Chambers, J. Q., Jenkins, H. S., Brenning, A., and Trumbore, S. E.: Recovery of Forest Structure Following 705 Large-Scale Windthrows in the Northwestern Amazon, *Forests*, 12, 667, <https://doi.org/10.3390/fl2060667>, 2021.
- Vepakomma, U., St-Onge, B., and Kneeshaw, D.: Spatially explicit characterization of boreal forest gap dynamics using multi-temporal lidar data, *Remote Sens. Environ.*, 112, 2326–2340, <https://doi.org/10.1016/j.rse.2007.10.001>, 2008.
- Vitousek, P. M. and Denslow, J. S.: Nitrogen and Phosphorus Availability in Treefall Gaps of a Lowland Tropical Rainforest, *J. Ecol.*, 74, 1167, <https://doi.org/10.2307/2260241>, 1986.
- 710 Whitmore, T. C.: Canopy Gaps and the Two Major Groups of Forest Trees, *Ecology*, 70, 536–538, <https://doi.org/10.2307/1940195>, 1989.

- Wu, J., Albert, L. P., Lopes, A. P., Restrepo-Coupe, N., Hayek, M., Wiedemann, K. T., Guan, K., Stark, S. C., Christoffersen, B., Prohaska, N., Tavares, J. V., Marostica, S., Kobayashi, H., Ferreira, M. L., Campos, K. S., Dda Silva, R., Brando, P. M., Dye, D. G., Huxman, T. E., Huete, A. R., Nelson, B. W., and Saleska, S. R.: Leaf development and demography explain photosynthetic seasonality in Amazon evergreen forests, *Science* (80-. ), 351, 972–976, <https://doi.org/10.1126/science.aad5068>, 2016.
- 715 Yavitt, J. B., Battles, J. J., Lang, G. E., and Knight, D. H.: The canopy gap regime in a secondary Neotropical forest in Panama, *J. Trop. Ecol.*, 11, 391–402, <https://doi.org/10.1017/S0266467400008853>, 1995.
- Yue, W., Juyu, L., Zhaochen, Z., Jianbo, H., Ji, Y., Yong, L., and Wanhui, Y.: Forest Plots Gap and Canopy Structure Analysis Based on Two UAV Images 帶地理, *Trop. Geogr.*, 39, 553–561, <https://doi.org/10.13284/j.cnki.rddl.003148>, 2019.
- 720 Zuleta, D., Arellano, G., Muller-Landau, H. C., McMahon, S. M., Aguilar, S., Bunyavejchewin, S., Cárdenas, D., Chang-Yang, C., Duque, A., Mitre, D., Nasardin, M., Pérez, R., Sun, I., Yao, T. L., and Davies, S. J.: Individual tree damage dominates mortality risk factors across six tropical forests, *New Phytol.*, 233, 705–721, <https://doi.org/10.1111/nph.17832>, 2022.
- Zuleta, D., Arellano, G., McMahon, S. M., Aguilar, S., Bunyavejchewin, S., Castaño, N., Chang-Yang, C., Duque, A., Mitre, 725 D., Nasardin, M., Pérez, R., Sun, I., Yao, T. L., Valencia, R., Krishna Moorthy, S. M., Verbeeck, H., and Davies, S. J.: Damage to living trees contributes to almost half of the biomass losses in tropical forests, *Glob. Chang. Biol.*, 1–12, <https://doi.org/10.1111/gcb.16687>, 2023.